Protonated Ions

DOI: 10.1002/anie.200802272

Dipositively Charged Protonated a_3 and a_2 Ions: Generation by Fragmentation of $[La(GGG)(CH_3CN)_2]^{3+}$**

*Tujin Shi, Chi-Kit Siu, K. W. Michael Siu, and Alan C. Hopkinson**

Iminium ions a_2 and a_3 are fragment ions in the gas-phase microsequencing of protonated peptides in proteomics.[1] Protonation of these small a_n ions as they are being formed during peptide fragmentation is, in theory, possible but has not hitherto been reported. This absence is presumably because of the Coulombic repulsion encountered by any given mobile proton in the vicinity of the incipient a_2 and a_3 ions, just prior to dissociation.[2] Herein, we report the first observation of a small, dipositive (and hence high-charge-density) protonated a_3 ion, $(a_3+H)^{2+}$, and a protonated a_2 ion, $(a_2+H)^{2+}$, produced through the tandem mass spectrometry of a triply charged lanthanum complex of triglycine (GGG).

The fragmentations of metal-ion cationized peptides, predominantly those of monocations (alkali metals,[3] Cu,[4] and Ag[5]) and dications (Ca,[6] Ni,[7a] Cu,[7a] and Zn[7]), have aroused much interest. For multicharged complexes, charge reduction by proton transfer is a common channel;[8] consequently, few $[M(peptide)]^{3+}$ (M = metal) complexes have been reported.[9] Recently, we observed the ions $[La(peptide)]^{3+}$, in which the peptide had either three or four residues, one of which was an arginine.[9b] The only complexes of peptides having amino acids with hydrocarbon side chains that were observed included solvent molecules, for example, $[La(GGG)(CH_3CN)_2]^{3+}$ (Scheme 1). Herein, we exploit the collision-induced dissociation (CID) of this complex, which leads to charge disproportionation and observation of $(a_3+H)^{2+}$ (**1**), and $[LaO(CH_3CN)]^+$ plus the neutrals CO and CH_3CN. Ion **1**, in turn, eliminates methanimine and CO to give $(a_2+H)^{2+}$ (**2**).

Figure 1 shows the CID of $[La(GGG)(CH_3CN)_2]^{3+}$ (m/z 136.7), the protonated a_3 ion, $(a_3+H)^{2+}$ (m/z 72.5), and its complementary ions $[LaO(CH_3CN)]^+$ (m/z 196) and $[LaO]^+$ (m/z 155) in the dissociation. The CID of the deuterium-labeled precursor ions $[La([D_5]GGG)(CD_3CN)_2]^{3+}$ and $[La(G(\alpha,\alpha\text{-}[D_2]G)G)(CH_3CN)_2]^{3+}$ confirmed the formation of $(a_3+H)^{2+}$, which was mass-shifted to m/z 75 and 73.5, respectively.

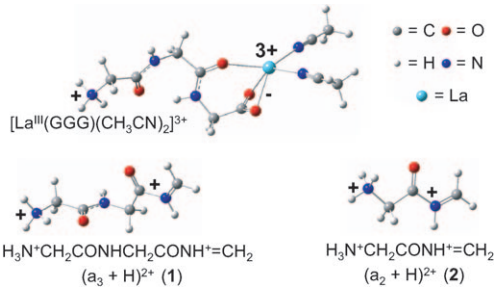

Scheme 1. Lowest-energy structures of $[La(GGG)(CH_3CN)_2]^{3+}$ and protonated a_3 (**1**) and a_2 (**2**) ions.

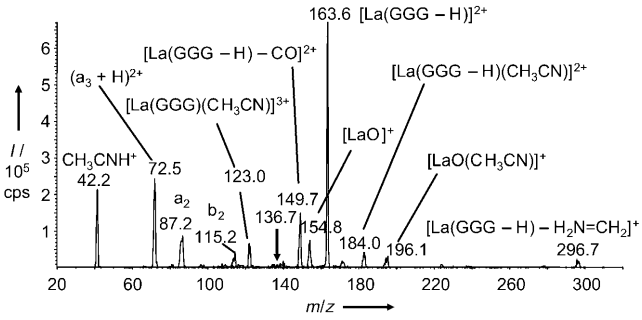

Figure 1. CID of $[La(GGG)(CH_3CN)_2]^{3+}$ (m/z 136.7) at E_{lab} = 30 eV. cps = counts per second.

Density functional theory (DFT) performed by the Gaussian 03 quantum-chemical calculation package[10a] shows that the preferred triglycine conformation in binding to La^{3+} is zwitterionic (Scheme 1). The formation of **1** after collisional activation of the complex is facilitated by the high affinity of La for O, which leads to cleavage of the carboxylate moiety and deposition of a second formal positive charge on the imino group of **1**. The lowest-energy fragmentation pathway has a barrier of 57.4 kcal mol^{-1} (Scheme 2). The intermediate ion $(b_3+H)^{2+}$ (**3**) is not evident in Figure 1, as the barrier to this ion is 52.5 kcal mol^{-1}, only 5 kcal mol^{-1} lower. Formation of **1** via $[La(GGG)(CH_3CN)]^{3+}$ (m/z 123) is noncompetitive because of a much larger barrier of 98.8 kcal mol^{-1}. However, the low-abundance $[La(GGG)(CH_3CN)]^{3+}$ formed does dissociate efficiently to give **1** (see Figure S1 in the Supporting Information).

As anticipated from its high charge density and, therefore, the large intramolecular Coulombic repulsion, the $(a_3+H)^{2+}$

[*] Dr. C.-K. Siu, Prof. K. W. M. Siu, Prof. A. C. Hopkinson
Department of Chemistry
Centre for Research in Mass Spectrometry, York University
4700 Keele Street, Toronto, ON, M3J 1P3 (Canada)
Fax: (+1) 416-736-5936
E-mail: ach@yorku.ca
Dr. T. Shi
Centre for Research in Neurodegenerative Diseases
University of Toronto, Toronto, ON, M5S 3H2 (Canada)

[**] This study was supported by the Natural Sciences and Engineering Research Council (NSERC) of Canada and made possible by the facilities of the Shared Hierarchical Academic Research Computing Network (SHARCNET: www.sharcnet.ca). We thank Dr. Julia Laskin for helpful discussions on the RRKM modeling.

Supporting information for this article is available on the WWW under http://dx.doi.org/10.1002/anie.200802272.

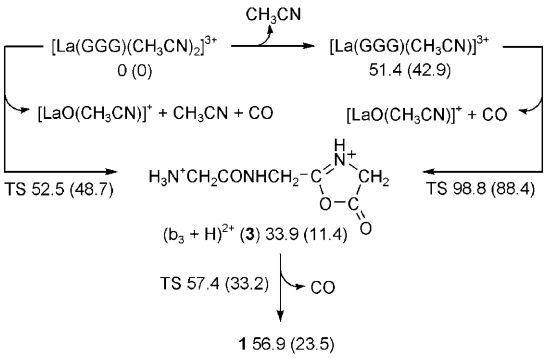

Scheme 2. Fragmentation pathways of $[La(GGG)(CH_3CN)_2]^{3+}$. Energies ΔH_0° (ΔG_{298}°) are in kcal mol^{-1}. TS = transition structure.

ion was fragile and dissociated facilely to give monopositive product ions (Figure 2a). The most abundant of these was the a_2 ion (m/z 87); of the minor products, only the $(b_2-NH_3)^+$ ion (m/z 98, see below) has not been reported in the CID of

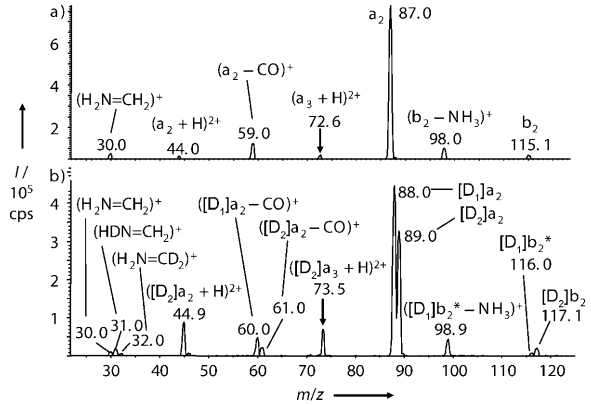

Figure 2. CID of a) $(a_3+H)^{2+}$ (**1**; m/z 72.6) and b) its isotopic analogue ($[D_2]a_3+H)^{2+}$ (m/z 73.5) generated from GGG and G(α,α-[D_2]G)G, respectively; collision energies at E_{lab} of 20 eV.

protonated triglycine.[11] Most significantly, the CID of $(a_3+H)^{2+}$ gave in low abundance the even smaller dipositive ion $(a_2+H)^{2+}$ (m/z 44). Note that the $(a_2+H)^{2+}$ ion formed from G(α,α-[D_2]G)G was shifted to m/z 45 (Figure 2b), as expected for a dipositive ion that carried two deuterium substitutions. Replacing the triglycine (GGG) with a trialanine (AAA) moiety gave the same fragmentation results; both $(a_3+H)^{2+}$ (m/z 93.6) and $(a_2+H)^{2+}$ (m/z 57.9) were formed (see Figure S4 in the Supporting Information). Furthermore, an experiment on the tripeptide GAA showed that the $(a_3+H)^{2+}$ ion (m/z 86.6) loses a neutral ethanimine and CO from the C-terminal end to generate $(a_2+H)^{2+}$ (m/z 50.8; see Figure S5 in the Supporting Information), thus establishing that the $(a_2+H)^{2+}$ ion contains the N-terminal and central residues.

Isotopic substitution with ^{15}N in the C-terminal residue established unambiguously that the formation of all the aforementioned ions from triglycine involved the loss of $(NH_2{=}CH_2)^+$ from the C-terminal residue (Figure S3b in the Supporting Information). The use of G(α,α-[D_2]G)G reveals additional novel ions (Figure 2b). The b_2 ions at m/z 117 and 116 (the latter hereafter designated as $[D_1]b_2$*) differ by one deuterium atom; importantly, only the $[D_1]b_2$* ion lost NH_3 to give the product ion at m/z 99. The identities of these ions and their subsequent secondary dissociation products as determined by DFT are given in Scheme 3 (see Figure S7 in the

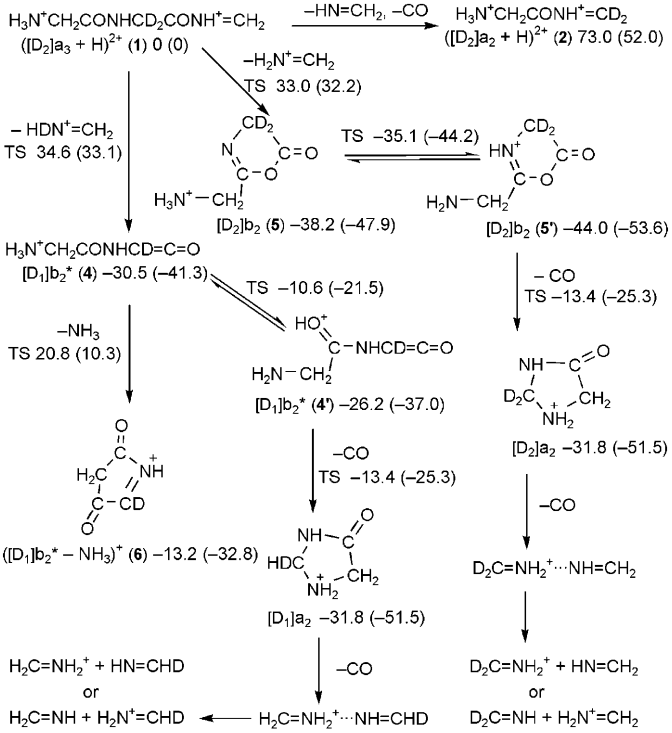

Scheme 3. Ions and their secondary dissociation products as determined by DFT. Energies ΔH_0° (ΔG_{298}°) are in kcal mol^{-1}.

Supporting Information for a detailed energy profile). The $[D_1]b_2$* ion (**4**) is a protonated ketene,[5a] and the $[D_2]b_2$ ion (**5**) is a protonated oxazolone.[11] Protonated oxazolones lose CO upon CID, not NH_3.[11] The $([D_1]b_2-NH_3)^+$ ion is most likely protonated 1-pyrroline-3,5-dione (**6**). These interpretations were corroborated by the dissociation of ion **1** from [D_5]GGG (see Figure S3a in the Supporting Information), which also gave two b_2 ions at m/z 119 and 118 and only one $(b_2-ND_3)^+$ ion at m/z 99, which implies that the m/z 119 ion was the protonated ketene, b_2*. The formation of ions **4** and **5** from ion **1** requires approximately and comparably 33–35 kcal mol^{-1} (Scheme 3).

Both the b_2 and b_2* ions lost CO (the latter after proton transfer to the amide oxygen atom (**4′**), then to the ketene carbon atom), which produced abundant cyclic a_2 ions (m/z 89 and 88) and proton-bound imine dimers (m/z 61 and 62) in lower abundances.[11e] For both the a_2 and imine dimer ions, the abundances of the monodeuterated isotopomers were higher than those of the dideuterated isomers, which indicates that the formation of b_2* was the major channel, but that this ion is more fragile. Further evidence for b_2* being the dominant channel was provided by the relative abundances of ions at m/z 30, 31, and 32 in Figure 2b. The most abundant of

the three had m/z 31, CNH_3D^+, which corresponds to the loss of $HDN^+{=}CH_2$ to form b_2* (Scheme 3). Formation of the dipositive ion **2** is endothermic by 73 kcal mol^{-1}, significantly larger than the barriers in the formation of monopositive ions. This finding corroborates the low abundances of $(a_2+H)^{2+}$ observed in Figure 2.

The kinetics of the three main fragmentation channels of $(a_3+H)^{2+}$ were modeled by employing the Rice–Ramsperger–Kassel–Marcus (RRKM) theory. The theoretical branching ratio for the channels of b_2* and b_2 formation is in agreement with the experimental energy-resolved CID results; the former channel is favored over the latter by a transition structure with a larger activation entropy. The formation of $(a_2+H)^{2+}$ is energetically unfavorable, but becomes kinetically competitive under higher collision energies. In addition, this dissociation channel is further enhanced under our experimental conditions in which the $(a_3+H)^{2+}$ ion has an average of 40 collisions (see the Supporting Information).

The mechanism for the generation of **2**, which involves cleavage of the C–N and C–C_α bonds at the amide linkage between the second and third residues of **1**, was examined by DFT molecular dynamics (MD) simulations employing the Car–Parrinello (CP)-based metadynamics (MTD) approach with which finite temperature effects are explicitly included in the equations of motion of the nuclei.[12] The reaction coordinates were defined by two collective variables (CVs), s(C–N) and s(C–C_α), which are continuous functions decreasing from 1 to 0 when a bond cleaves. After an equilibrating MD run at a temperature of 300 K (about 2 ps), the dynamics of **1** was biased with a history-dependent potential in a space defined by the CVs, $V(s(\text{C–N}),s(\text{C–C}_\alpha))$, until the dissociation occurred. The potential V gave a two-dimensional free energy surface for the reaction (Figure 3). The ion **1**, initially located at the well-defined minimum around $V(1,1)$, undergoes C–N bond cleavage with a free-energy barrier of 35 kcal mol^{-1} to eliminate a $HN{=}CH_2$ molecule and form $(b_2+H)^{2+}$, an ion at the local minimum around $V(0,1)$ with a free energy 30 kcal mol^{-1} above **1**. The $(b_2+H)^{2+}$ ion is not observed in our CID spectra and readily loses a CO molecule to form **2** $V(0,0)$.

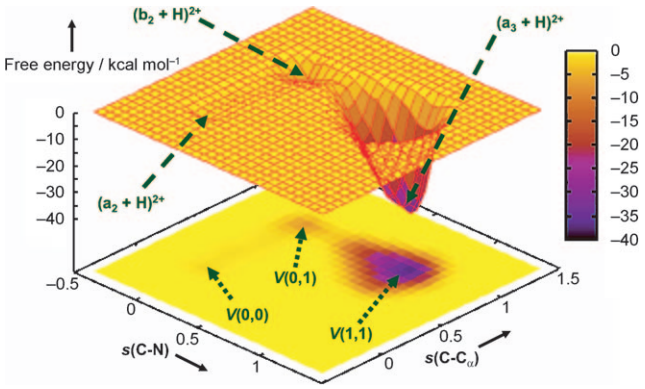

Figure 3. Free energy surface of $(a_3+H)^{2+}$ simulated by using CP-MTD at 300 K.

In conclusion, a novel, small, and doubly protonated fragment, the ion $(a_3+H)^{2+}$, has been generated in a mass spectrometer by CID of $[La(GGG)(CH_3CN)_2]^{3+}$. This $(a_3+H)^{2+}$ ion was fragile and underwent highly exothermic charge separation reactions to form the $(H_2N{=}CH_2)^+$ ion from the C-terminal end and two types of b_2 ions, protonated oxazolone and amino-protonated ketene. The former b_2 ion followed the canonical fragmentation pathway to give an a_2 ion by losing a CO molecule, whereas the latter b_2* ion lost CO to give an a_2 ion or lost NH_3 to give protonated 1-pyrroline-3,5-dione. An even smaller doubly protonated a_2 ion, $(a_2+H)^{2+}$, was produced in the CID of $(a_3+H)^{2+}$ by losing two neutral fragments, CO and $HN{=}CH_2$, both from the C-terminal end. The mechanisms of all these fragmentation reactions were deduced and corroborated by isotope-labeling experiments, DFT, and CP-based MTD. The generation of a peptide fragment with two positive charges on the backbone, one at the N-terminal ammonium group and the other at the C-terminal iminium group, is potentially useful for minimizing scrambling in the primary structure resulting from cyclization, a process leading to the formation of macrocyclic b_n and a_n peptide fragment ions.[13] The generality of this route to these unusual dipositive peptide fragment ions will be explored by examining the fragmentations of other $[La(peptide)(CH_3CN)_n]^{3+}$ ions.

Experimental Section

Experiments were performed on an MDS SCIEX (Concord, ON) API 3000 prototype triple-quadrupole mass spectrometer. The complex ion was generated by electrospraying tripeptide GGG (1 mM) + $La(NO_3)_3$ (0.1 mM) in H_2O/CH_3CN (1:1) solution. Isotopically labeled triglycines were used, including deuterium labels for the exchangeable hydrogen atoms, $[D_5]$GGG, and for the α-hydrogen atoms of the second residue, G(α,α-$[D_2]$G)G, and ^{15}N labels for the C-terminal residue, GG($[^{15}N]$G).

The static geometry optimizations and harmonic vibrational frequency analyses for all minima and transition structures were performed with the Gaussian 03 package[10a] employing the B3LYP hybrid DFT functional.[10b,c] The 6-31++G(d,p) basis set[10d,e] for the main-group elements and the Stuttgart/Cologne relativistic effective core potential basis set[10f,g] for the metal were used to study the fragmentation mechanism of the lanthanum complex, and the 6-311++G(d,p) basis set[10d,e] was used for the fragmentation mechanism of **1**.

In the CPMD[12] simulations, an ion was placed in a cubic box with dimensions of 16 Å^3. The energy was evaluated by using the HCTH/120 DFT functional.[12d] Troullier–Martins pseudopotentials[12e] were used and the wave functions were expanded by a plane-wave basis set with an energy cutoff of 70 Ry. The endothermicity for the formation of **2** by eliminating CO and $NH{=}CH_2$ from **1** calculated with the CPMD package (80 kcal mol^{-1}) is almost identical to that with the Gaussian 03 package at the B3LYP/6-311++G(d,p) level without zero-point energy correction (79.6 kcal mol^{-1}).

In the MTD simulations,[12b,c] the equations of motion were integrated with a time step of 4 atomic units (0.097 fs) and a fictitious electron mass of 500 amu. The CV was defined by a continuous function, $s(r)=(1-(r/r_c)^p)/(1-(r/r_c)^q)$, where r is the interatomic distance of C–N or C–C_α, $r_c=1.8$ Å, $p=6$, and $q=12$, with a mass $M_i=50$ and a coupling force constant $k_i=3$. A biasing Gaussian potential V was applied every 50–110 MD steps determined by a tolerance of 0.005 for the acceptance of a new MTD step. The shape of V was defined by a constant width $\Delta s_i^{\perp}=0.05$ a.u. and a variable

height $W = 0.001$–0.01 a.u. tuned automatically according to the curvature of the underlying potential.

Received: May 15, 2008
Revised: July 31, 2008
Published online: September 24, 2008

Keywords: density functional calculations · iminium ions · mass spectrometry · molecular dynamics · peptides

[1] R. Aebersold, D. R. Goodlett, *Chem. Rev.* **2001**, *101*, 269.
[2] G. Tsaprailis, H. Nair, Á. Somogyi, V. H. Wysocki, W. Zhong, J. H. Futrell, S. G. Summerfield, S. J. Gaskell, *J. Am. Chem. Soc.* **1999**, *121*, 5142.
[3] a) L. M. Teesch, J. Adams, *J. Am. Chem. Soc.* **1991**, *113*, 812; b) S. W. Lee, H. S. Kim, J. L. Beauchamp, *J. Am. Chem. Soc.* **1998**, *120*, 3188; c) T. Lin, A. H. Payne, G. L. Glish, *J. Am. Soc. Mass Spectrom.* **2001**, *12*, 497; d) W. Y. Feng, C. Gronert, K. A. Fletcher, A. Warres, C. B. Lebrilla, *Int. J. Mass Spectrom.* **2003**, *222*, 117; e) V. Anbalagan, J. N. Patel, G. Niyakorn, M. J. Van Stipdonk, *Rapid Commun. Mass Spectrom.* **2003**, *17*, 291; f) K. A. Newton, S. A. McLuckey, *J. Am. Soc. Mass Spectrom.* **2004**, *15*, 607.
[4] a) S. J. Shields, B. K. Bluhm, D. H. Russell, *Int. J. Mass Spectrom.* **1999**, *182–183*, 185; b) S. J. Shields, B. K. Bluhm, D. H. Russell, *J. Am. Soc. Mass Spectrom.* **2000**, *11*, 626.
[5] a) V. W. M. Lee, H. B. Li, T. C. Lau, K. W. M. Siu, *J. Am. Chem. Soc.* **1998**, *120*, 7302; b) I. K. Chu, X. Guo, T. C. Lau, K. W. M. Siu, *Anal. Chem.* **1999**, *71*, 2364; c) H. B. Li, K. W. M. Siu, R. Guevremont, J. C. Y. LeBlanc, *J. Am. Soc. Mass Spectrom.* **1997**, *8*, 781; d) I. K. Chu, T. Shoeib, X. Guo, C. F. Rodriquez, T. C. Lan, A. C. Hopkinson, K. W. M. Siu, *J. Am. Soc. Mass Spectrom.* **2001**, *12*, 163; e) V. Anbalagan, B. A. Perera, A. T. M. Silva, A. L. Gallardo, M. Barber, J. M. Barr, S. M. Terkarli, E. R. Talaty, M. J. Van Stipdonk, *J. Mass Spectrom.* **2002**, *37*, 910; f) I. K. Chu, D. M. Cox, X. Guo, I. Kireeva, T. C. Lau, J. C. McDermott, K. W. M. Siu, *Anal. Chem.* **2002**, *74*, 2072.
[6] O. V. Nemirovskiy, M. L. Gross, *J. Am. Soc. Mass Spectrom.* **1998**, *9*, 1020.
[7] a) P. F. Hu, J. A. Loo, *J. Am. Chem. Soc.* **1995**, *117*, 11314; b) J. A. Loo, P. F. Hu, R. D. Smith, *J. Am. Soc. Mass Spectrom.* **1994**, *5*, 959.
[8] a) A. T. Blades, P. Jayaweera, M. G. Ikonomou, P. Kebarle, *Int. J. Mass Spectrom. Ion Process.* **1990**, *101*, 325; b) Z. L. Cheng, K. W. M. Siu, R. Guevremont, S. S. Berman, *Org. Mass Spectrom.* **1992**, *27*, 1370; c) N. R. Walker, R. R. Wright, A. J. Stace, C. A. Woodward, *Int. J. Mass Spectrom.* **1999**, *188*, 113; d) D. Vukomanovic, J. A. Stone, *Int. J. Mass Spectrom.* **2000**, *202*, 251.
[9] a) A. A. Shvartsburg, R. C. Jones, *J. Am. Soc. Mass Spectrom.* **2004**, *15*, 406; b) T. Shi, K. W. M. Siu, A. C. Hopkinson, *J. Phys. Chem. A* **2007**, *111*, 11562.
[10] a) M. J. Frisch et al., Gaussian 03 D.01, Gaussian, Inc., Wallingford, CT, **2004**; b) A. D. Becke, *J. Chem. Phys.* **1993**, *98*, 5648; c) C. Lee, W. Yang, R. G. Parr, *Phys. Rev. B* **1988**, *37*, 785; d) W. J. Hehre, R. Ditchfield, J. A. Pople, *J. Chem. Phys.* **1972**, *56*, 2257; e) T. Clark, J. Chandrasekhar, G. W. Spitznagel, P. von R. Schleyer, *J. Comput. Chem.* **1983**, *4*, 294; f) M. Dolg, H. Stoll, A. Sovin, H. Preuss, *Theor. Chim. Acta* **1989**, *75*, 173; g) X. Cao, M. Dolg, *J. Chem. Phys.* **2001**, *115*, 7348.
[11] a) T. Yalcin, C. Khouw, I. G. Csizmadia, M. B. Peterson, A. G. Harrison, *J. Am. Soc. Mass Spectrom.* **1995**, *6*, 1165; b) A. G. Harrison, A. B. Young, C. Bleiholder, S. Suhai, B. Paizs, *J. Am. Chem. Soc.* **2006**, *128*, 1036; c) N. C. Polfer, J. Oomens, S. Suhai, B. Paizs, *J. Am. Chem. Soc.* **2005**, *127*, 17154; d) N. C. Polfer, J. Oomens, S. Suhai, B. Paizs, *J. Am. Chem. Soc.* **2007**, *129*, 5887; e) H. E. Aribi, C. F. Rodriquez, D. R. P. Almeida, Y. Ling, W. W. N. Mak, A. C. Hopkinson, K. W. M. Siu, *J. Am. Chem. Soc.* **2003**, *125*, 9229; f) H. El Aribi, G. Orlova, C. F. Rodriquez, D. R. P. Almeida, A. C. Hopkinson, K. W. M. Siu, *J. Phys. Chem. B* **2004**, *108*, 18743.
[12] a) R. Car, M. Parrinello, *Phys. Rev. Lett.* **1985**, *55*, 2471; b) A. Laio, M. Parrinello, *Proc. Natl. Acad. Sci. USA* **2002**, *99*, 12562; c) M. Iannuzzi, A. Laio, M. Parrinello, *Phys. Rev. Lett.* **2003**, *90*, 238302; d) F. A. Hamprecht, A. J. Cohen, D. J. Tozer, N. C. Handy, *J. Chem. Phys.* **1998**, *109*, 6264; e) N. Troullier, J. L. Martins, *Phys. Rev. B* **1991**, *43*, 1993.
[13] a) J. Yagüe, A. Paradela, M. Ramos, S. Ogueta, A. Marina, F. Barahona, J. A. López de Castro, J. Vázquez, *Anal. Chem.* **2003**, *75*, 1524; b) B. Paizs, S. Suhai, *Mass Spectrom. Rev.* **2005**, *24*, 508; c) A. G. Harrison, A. B. Young, C. Bleiholder, S. Suhai, B. Paizs, *J. Am. Chem. Soc.* **2006**, *128*, 10364; d) N. C. Polfer, J. Oomens, S. Suhai, B. Paizs, *J. Am. Chem. Soc.* **2007**, *129*, 5887; e) N. C. Polfer, B. C. Bohrer, M. D. Plasencia, B. Paizs, D. E. Clemmer, *J. Phys. Chem. A* **2008**, *112*, 1286; f) I. Riba-Garcia, K. Giles, R. H. Bateman, S. J. Gaskell, *J. Am. Soc. Mass Spectrom.* **2008**, *19*, 609.

